A High-Frequency AC Generator with High Gain Powered by 3.7 V Battery for Tumor Treating Fields

Yanpeng Lv[1], Shihan Lu[1], Yuqi Wang[2], Xuan Liu[1], and Jianhua Zhang[1]

[1]Zhengzhou University School of Electrical and Information Engineering
[2]Schneider Electric SA

February 10, 2025

Abstract

High-frequency AC field (100-300 kHz), which could generate tumor treating fields (TTFields) has been FDA-approved for glioblastoma multiforme (GBM) treatment. How to design a high-frequency AC field with low input battery (3.7 V) power is important for outdoor stimulation with a long treatment time.This study utilizes an LCLC step-up resonant circuit integrated with a linear isolated transformer (LCLLC) to generate a 200 kHz AC field using low DC input. Theoretical circuit analysis investigated the excitation inductance's impact on voltage gain under capacitive bio-loads. An experimental prototype was developed based on selected parameters, generating 200 kHz AC waveforms (66 V output, voltage gain: 17.8) with 5.1 W input power from a 3.7 V battery, sustaining 8.7-hour operation. Coupled insulated electrodes demonstrated high-efficacy AC field delivery. CCK-8 assays confirmed that generator stimulation significantly inhibited U251 glioblastoma cell proliferation. The theoretical analysis showed that the adjustment of excitation inductance of linear isolated transformer in LCLLC circuit could benefit to achieve a high voltage gain with low input power. This work developed a low-power 200 kHz AC field generator powered by 3.7 V DC batteries, achieving high voltage gain (17.8) and significant cell proliferation inhibition, enabling portable tumor-treating field applications.

A High-Frequency AC Generator with High Gain Powered by 3.7 V Battery for Tumor Treating Fields

Yanpeng Lv[1], Shihan Lu[1], Yuqi Wang[2], Xuan Liu[1], Jianhua Zhang[1]

[1] School of Electrical and Information Engineering, Zhengzhou University, Zhengzhou, 450001, China.

[2] IA China Hub, Schneider Electric SA, Wuxi 214028, China

Corresponding Author: Yanpeng Lv (yanpenglv@foxmail.com)

Abstract High-frequency AC field (100-300 kHz), which could generate tumor treating fields (TTFields) has been FDA-approved for glioblastoma multiforme (GBM) treatment. How to design a high-frequency AC field with low input battery (3.7 V) power is important for outdoor stimulation with a long treatment time.This study utilizes an LCLC step-up resonant circuit integrated with a linear isolated transformer (LCLLC) to generate a 200 kHz AC field using low DC input. Theoretical circuit analysis investigated the excitation inductance's impact on voltage gain under capacitive bio-loads. An experimental prototype was developed based on selected parameters, generating 200 kHz AC waveforms (66 V output, voltage gain: 17.8) with 5.1 W input power from a 3.7 V battery, sustaining 8.7-hour operation. Coupled insulated electrodes demonstrated high-efficacy AC field delivery. CCK-8 assays confirmed that generator stimulation significantly inhibited U251 glioblastoma cell proliferation. The theoretical analysis showed that the adjustment of excitation inductance of linear isolated transformer in LCLLC circuit could benefit to achieve a high voltage gain with low input power. This work developed a low-power 200 kHz AC field generator powered by 3.7 V DC

batteries, achieving high voltage gain (17.8) and significant cell proliferation inhibition, enabling portable tumor-treating field applications.

Keywords: high-frequency AC field, tumor treating fields, cell proliferation inhibition, high voltage gain, resonant circuit

Introduction

Glioblastoma multiforme (GBM) is a highly aggressive and invasive brain tumor. The World Health Organization (WHO) classifies grade IV glioma as the most severe form of central nervous system disease. The median survival rate ranges from 14.6 to 16.7 months, with a five-year survival rate of merely 5%, even with treatments such as surgery, radiation therapy, and chemotherapy [1]. Consequently, developing effective therapies for GBM remains a significant challenge. Recent studies have demonstrated the potential of electric fields in cancer treatment. Tumor Treating Fields (TTFields), utilizing high-frequency alternating current (AC) fields (100-300 kHz), have shown efficacy in tumor treatment [2-3]. *In vitro* studies indicate that TTFields can inhibit cell proliferation at intensities of 1-3 V/cm. TTFields are hypothesized to disrupt or delay cell division during early mitotic phases. During cytokinesis, TTFields may induce dielectrophoretic forces that displace polarizable macromolecules and ions toward the furrow, causing membrane blebbing and subsequent cell death [4-5]. TTFields have been clinically validated as an adjuvant therapy to chemotherapy in GBM treatment and have received FDA approval as a monotherapy for recurrent GBM. The Optune system, developed by Novocure Ltd., generates TTFields for clinical administration. Clinical trials demonstrated a median overall survival of 20.5 months (16.7-25.0 months) for TTFields combined with temozolomide, significantly longer than the 15.6 months (13.3-19.1 months) observed with temozolomide alone [6]. TTFields shows a promising adjuvant therapy for GBM treatment. Effective TTFields treatment requires high-frequency AC fields (100-300 kHz) with intensities of 1-3 V/cm. However, few studies have addressed the design of TTFields delivery devices. For research experiment, the protocol that oscillator or an AC generator, connected to a high voltage amplifier is usually used to produce AC field with high frequency in the range from 100 kHz to 300 kHz. In general, Novocure Ltd. also used this protocol to generate AC field for TTFields experiment by lab researchers [7-9]. Due to the conflict of interest, they did not open the structure of clinical apparatus. Optune apparatus consists of the transducer arrays with insulated electrodes, electric field generator (set at a frequency of 200 kHz) and battery. Patients receive TTFields via four transducer arrays delivering 200 kHz electric fields to the brain. Each transducer array delivers currents ranging from 400 to 1000 mA, typically 900 mA, with head impedance values between 58.6 and 91.2 Ω. The system generates voltages exceeding 50 V and power outputs around 50 W [10-12]. The use of insulated electrodes creates predominantly capacitive impedance, resulting in displacement currents through the head. However, the output power is constrained by the limitations of high-voltage amplifiers. For instance, generating 50 V AC fields requires matching DC power supplies, with average power consumption reaching at least 36 W when delivering 1000 mA currents. These technical constraints pose challenges for developing portable clinical devices with stable high-power outputs. With advancements in power electronics, DC/AC inverters have become widely adopted in industrial applications including induction heating systems, communication networks, and uninterruptible power supplies [13-21]. A typical DC/AC inverter comprises a full-bridge inverter and a resonant tank utilizing PWM control. The full-bridge inverter generates rectangular pulses, while resonant step-up topologies (LLC/LCC/LCLC) serve dual functions: filtering to produce AC waveforms and voltage boosting through high-ratio line-frequency transformers [22-26]. For instance, Blinov et al. developed a 50 kHz DC/AC inverter converting 40 V DC to 230 V AC for telecommunications [27], while Kummari et al. demonstrated a DC/AC inverter achieving 325 V AC output [28]. High-power DC/AC inverters for UPS and battery systems typically combine low-voltage SPWM circuits with line-frequency transformers for voltage amplification [29-30]. High-frequency AC fields (100-300 kHz) constitute the operational foundation of TTFields devices. Although DC/AC inverters represent a viable topology for therapeutic high-frequency AC field generation, PWM control becomes impractical at therapeutic frequencies (>2 MHz) due to excessive switching losses. Resonant step-up converters (LLC/LCC/LCLC) offer dual advantages: extracting

fundamental frequency components from rectangular pulses while providing voltage gain. Standard 3.7 V lithium batteries provide portable high-current DC sources suitable for outdoor TTFields operation, addressing the Optune system's requirement for supplemental batteries during mobile use exceeding one hour [31]. Developing 3.7 V-powered inverters with optimized high-gain/high-frequency characteristics remains critical for portable TTFields implementation. Notably, no prior studies have reported TTFields generation using capacitive-impedance DC/AC inverters. At therapeutic frequencies, capacitive impedance may interact with resonant converters, potentially compromising voltage output. This work implements a 3.7 V-powered full-bridge inverter with resonant tank to generate 200 kHz therapeutic fields. An LCLLC topology was developed by integrating a 1:1 line transformer into the LCLC converter, achieving 17.8× voltage gain (66.0 V). Theoretical analysis guided parameter selection for the modified circuit, where transformer excitation inductance was optimized to align the operating frequency with the primary resonance. A prototype employing four parallel 3.7 V/3200 mAh batteries successfully generated 200 kHz waveforms, maintaining stable AC output for 8.7 hours suitable for extended outdoor use. This study showed an easy-implemented topology with a voltage regulation to design the TTFields apparatus.

Principle and Analysis of Operation of LCLLC Resonant Boost Converter

Main Circuit Topology & Equivalent Model of the LCLLC Circuit

The study utilizes an LCLC resonant tank to step up the AC waveform voltage with the goal of increasing the effective voltage for tumor treatment. To achieve further voltage multiplication, the LCLC resonant tank is modified by adding a 1:1 transformer, referred to as LCLLC in this study. Fig. 1a illustrates the proposed DC/AC inverter with the LCLLC resonant boost tank, which primarily consists of a 3.7 V DC battery power supply (V_{in}), H-bridge switches (S_1 to S_4) and the energy storage capacitors C_s . The voltage, V_s , from the H-bridge passes through the LCLLC resonant tank to achieve high voltage gain.

Hosted file

`image1.emf` available at https://authorea.com/users/890168/articles/1267414-a-high-frequency-ac-generator-with-high-gain-powered-by-3-7-v-battery-for-tumor-treating-fields

Fig. 1 (a) The main circuit topology of DC/AC inverter with LCLLC resonant boost tank. (b) The simplified equivalent circuit of the LCLLC resonant circuit.

The simplified ideal equivalent circuit of the resonant inverter is shown in Fig. 1b [33-36]. Assumed that the isolated transformer with ratio of 1:1 is an ideal component, which is considered as an ideal inductance. Therefore, LCLC circuit with adding an excitation inductance (LCLLC) was analyzed. A rectangular bipolar pulse was generated through the full-bridge inverter, which can be expressed via Fourier decomposition in the following equation:

The equation defines n as a natural number and ω as the switching angular frequency of the full-bridge inverter, with a square wave amplitude of A. According to this equation, V_s contains only odd harmonics, such as the 3rd, 5th, and 7th, etc. By filtering out the higher harmonics and amplifying the fundamental component, the desired sinusoidal AC voltage output is achieved.

Based on the circuit in Fig. 1b, according to the Kirchhoff's law of voltage and current, the output voltage can be listed as Eq. (2):

The voltage gain is derived in the following equation:

The Analysis of the LCLLC Circuit

Assumed that the L_t is approaching infinity, the circuit can be considered as an LCLC topology and the voltage gain can be simplified by the following equation:

As previously stated in the introduction, the bio-load by TTFields is a capacitive impedance. The First Harmonic Approximation (FHA) analysis offers a valuable reference for the selection of parameters for LCLC circuit structures without significantly high-order harmonics [37]. A preliminary parameter selection with L_r = 6.8 μH, L_m = 22 μH, C_p =100 nF, C_w =10 nF is obtained based on parameter selection method of reference [37]. The load impedance chooses 90 Ω. Fig. 2a shows the voltage gain G with the variations of frequency at the load (Z_{load}) of 90 Ω. As shown in Fig. 2a, the attenuation multiplier at the third harmonic of the target frequency (600 kHz) has already reached to -32.1 dB. The voltage gain shows a bimodal distribution with frequency change:f_{p1} (167 kHz) and f_{p2} (287 kHz) are the two resonant gain frequencies. Fig. 2a shows that the LCLC circuit designed in this study could output 200 kHz AC field with high order harmonic.

Fig. 2a indicates that the voltage gain does not reach the maximum value at the target frequency (200 kHz). In order to obtain higher voltage gain, one way is that the target frequency could be shifted near the first resonant frequency by parameter sweeps ofL_r on the condition without high-order harmonics. Fig. 2b shows the frequency response of the voltage gains with different values of L_r . The L_r varies in the range form 0.1 μH to 100 μH. The first resonant frequency is gradually moved left with increased value ofL_r . For L_r of 1 μH, the first resonant frequency is 241 kHz. However, the voltage gain of third harmonics reaches -6.27 dB, which means that the high order harmonics may occur. The first resonant frequency is shifted from 241 kHz to 46 kHz, when the values of L_r range from 1 μH to 100 μH.

To choose the proper L_r to make target frequency shift to first resonant frequency, a least-square fitting is simply used to process the simulated data between first resonant frequency and values of L_r *(R^2* is 0.995*)* . The mathematical function is as follow:

Where the variable F represents the first resonant frequency (kHz). Based on the above mathematical function, the target frequency (200 kHz) could be shifted to first resonant frequency whenL_r is 4.1 μH.

Since the excitation inductance of transformer also involves the resonant step-up tank (Eq. (3)), this paper also tries to adjust the excitation inductance to shift the first resonant frequency, which is shown in Fig. 2c The L_t also varies in the range form 0.1 μH to 100 μH. The first resonant frequency is also gradually moved left with increased value of L_t . The first resonant frequency is shifted from 248 kHz to 171 kHz, when the values of L_t range from 1 μH to 100 μH. The adjustment of excitation inductance of transformer could also shift the targeted frequency to the first resonant frequency. Moreover, compared with the results on the adjustment of L_t *(Fig. 2b)* , the first resonant frequency changes in a relatively narrow change.

A least-square fitting is also used to process the simulated data between first resonant frequency and values ofL_t . The mathematical function is as follow*(R^2* is 0.986*)* :

Hosted file

`image11.emf` available at https://authorea.com/users/890168/articles/1267414-a-high-frequency-ac-generator-with-high-gain-powered-by-3-7-v-battery-for-tumor-treating-fields

Fig. 2 (a) A case study of gain with frequency variation for excitation inductance L_t=[?]. (b) The gain curve as a function of frequency for different inductances L_r for LCLLC circuit. (c) The output gain as a function of frequency for different inductance L_t for LCLLC circuit. (d) The fitting results on the first resonant frequency F as a function of the different inductance. The R^2 is 0.986 of the LCLLC structure and 0.995 of the LCLC structure, respectively. (e) The resonant gain of LCLC&LCLLC circuits at the frequency of 200kHz. (f) The gain relationship between the different transformer inductances L_t corresponding to the different capacitive loads at the target frequency of 200 kHz.

Based on Eq. (6), the target frequency (200 kHz) could be shifted to first resonant frequency when L_t is 10.5 μH. Fig. 2d indicates a compared study between the fitted curve between Eq. (5) (adjusting L_r , named

LCLC) and Eq. (6) (adjusting L_t , named LCLLC). The descending rate near 200 kHz by LCLLC is lower than that by LCLC. T*he* attenuation rate (0.90) is similar with the result by adjustment of L_r *(0.928). However, coefficient of* attenuation term by adjustment of L_t (74.31) is lower than that by adjustment of L_r *(200). Moreover, the curve by LCLLC with adjusting* excitation inductance of transformer shows a slow change *near the targeted frequency (200 kHz), while a relatively large change for LCLLC with adjusting inductance of first* resonant frequency. Fig. 2d demonstrates that with a large range of excitation inductances, the resonant frequency changes in a relatively narrow change, which indicates that fine turning of excitation inductance of transformer is a proper way to shift targeted frequency to resonant frequency.

Fig. 2e shows the voltage gain for LCLC and LCLLC resonant step-up tanks when the same targeted frequency (200 kHz) is first resonant frequency. The L_r is 4.1 μH for LCLC circuit, whileL_t is 10.5 μH for LCLLC circuit. Fig. 2e shows that the voltage gain of the LCLLC circuit structure is 72.91 dB, compared to 52.24 dB for the LCLC circuit. Furthermore, the voltage gain of third harmonic (600 kHz) is only -32 dB, which is also lower than that by LCLC (-27dB).

The above theoretical analysis showed a simple way to select parameters of resonant step-up tank. First, the tentative parameters of step-up tank based on the targeted resonant frequency and voltage gain. Then, the parameter sweeps of L_t (excitation inductance of transformer) was employed on the condition without high-order harmonics. The least-square fitting is also used to process the simulated data between first resonant frequency and values ofL_t . Finally, an adaptive commercial excitation inductance of transformer is selected to shift targeted frequency to resonant frequency, then boost the output voltage.

Due to the individual difference, the capacitive bio-load by TTFields also changes in a certain range, which could interference the resonant step-up converter, then affect output voltage. Since the bio-load is a capacitive impedance for TTField treatment, which could involves the resonant step-up tank. Fig. 2f shows the voltage gain with capacitive impedance change. With proper selction of excitation inductance, the maximum voltage gain at resonant frequency can be also achieved with proper excitation inductance for bio-loads with 60-90 Ω.

Miniaturized High Frequency AC Generator Construction

Simulation on High Frequency AC Generator

A DC-AC converter with a full-bridge inverter and LCLLC resonant tank are modeled and simulated using PSpice software based on the above theoretical analysis and parameters selection, which is shown in Fig. 3a. The detailed parameters of the resonant converter are listed in Table 1. This study aims to generate a 200 kHz AC waveform (above 50 V) using a regular lithium battery, utilizing a 3.7 V DC supply for the simulation. As shown in Fig. 3b, the output AC waveform generated by the LCLC structure is 33.6 V, while the LCLLC structure produces 53.8 V. The voltage gain for the LCLC structure is only 9.08, whereas the LCLLC structure achieves a gain of 14.54 (Fig. 3b).**Table 1** Design Parameter of the Proposed Resonant Converter

Symbol	Parameter	Value
f	Resonant frequency	200 kHz
L_{r1}	First resonant inductor for LCLC	4.1 μH
L_{r2}	First resonant inductor for LCLLC	6.8 μH
L_m	Second resonant inductor	22 μH
C_p	First resonant capacitor	100 nF
C_w	Second resonant capacitor	10 nF
Z_{load}	Load capacitance	8.7 nF
n	Transformer turn ratio	1:1
L_t	Inductance for LCLC circuit topology	[?]

L_{t1}	Primary side inductance of transformer	10.5 μH
L_{t2}	Inductance of the secondary side of the transformer	10.5 μH
V_{DC}	Input DC Voltage	3.7 V
C_s	Energy storage capacitors	680 μF

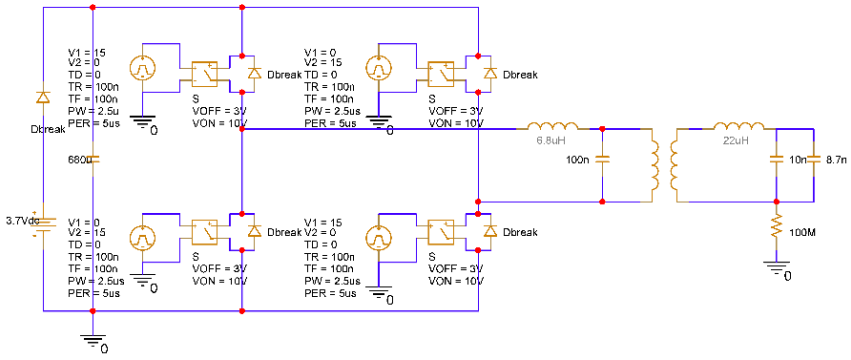

Fig. 3 (a) The circuit simulation model in PSpice. (b) The output voltage generated by both LCLC and LCLLC structures. (c) Input DC voltage and current for both LCLC and LCLLC structure. (d) Output AC voltage and current. (e) Comparisons of peak output voltage with and without transformer adjustment.

Fig. 3c illustrates the simulated input and output voltages and currents of both structures, showing that the LCLC structure requires a 5.1 V DC input to generate a 50.0 V AC waveform with an average power consumption of 17.95 W, whereas the LCLLC structure achieves the same output with a much lower average power of 5.22 W. Thus, the LCLC structure consumes about 3.44 times more power than the LCLLC structure. Additionally, Fig. 3c indicates the LCLLC structure needs lower input power to generate the TTFields waveform compared with the LCLC structure. Fig. 3d shows the output AC voltage and current.

As mentioned in the Introduction, the capacitive impedance of the patient's head during TTFields treatment at 200 kHz ranges from 58.6 to 91.2 Ω. Fig. 3e shows the output voltage V_p for the LCLLC structure at capacitive impedances of 60, 75, and 90 Ω. It was observed that V_p increases as impedance rises in the LCLLC structure. Fig. 3e shows that voltage gain varies with different transformer inductances. Therefore, this study adjusts the transformer inductance to stabilize the output voltage while maintaining the LCLLC structure. For 60 Ω impedance, the transformer inductance is set to 5 μH to achieve an output voltage above 50.0 V. With proper transformer inductance adjustment, the output voltage remains stable (54.0 V) across different capacitive impedances without altering the structure.

Experimental Test on High Frequency AC Prototype

Fig. 4 shows high frequency AC prototype, consisting of full-bridge inverter and LCLLC resonant tank. The Transistor-Transistor Logic (TTL) trigger signal of switch was provided by the FPGA core board (EP4CE6F17C8, Altera Corporation). The clock of 100 MHz was used to generate the TTL signals. Each MOSFET in a full-bridge inverter was driven by a driver circuit. In a driver circuit, the trigger signal was received by a high-speed optocoupler chip (HCPL-7710, AVAGO Corporation). Then, the signal was sent to a gate driver chip (IXDN609PI, IXYS Corporation), which boosted the TTL signal voltage to 15 V, then drove the MOSFET via some auxiliary circuits. In this study, a DC power supply employed four 3.7 V lithium batteries with a power output of 48 Wh. The on-time of each bridge arm is set to 2.16 μ s and the dead-time is set to 0.34 μ s. The proposed prototype is built to verify the theoretical analysis and simulation results. The detailed parameter selection is shown in Table 2. (In practical applications, there inevitably exist some discrepancies in the precision of the components).

Hosted file

image33.emf available at https://authorea.com/users/890168/articles/1267414-a-high-frequency-ac-generator-with-high-gain-powered-by-3-7-v-battery-for-tumor-treating-fields

Fig. 4 Experimental setup configuration: (a) Full-bridge inverter circuit and *LCLLC* resonant tank. (b) Power and FPGA

Table 2 Design Parameters of the Proposed Resonant Converter

Symbol	Parameter	Value
f	Resonant frequency	200 kHz
L_r	First resonant inductor	6.8 μH
L_m	Second resonant inductor	22 μH
C_p	First resonant capacitor	100 nF
C_w	Second resonant capacitor	10 nF
Z_{load}	Load capacitance	8.7 nF
n	Transformer turn ratio	1:1
L_{t1}	Primary side inductance of transformer	10 μH
L_{t2}	Inductance of the secondary side of transformer	10 μH
V_{DC}	Input DC Voltage	3.7 V
C_s	Energy storage capacitor	680 μF

Hosted file

image35.emf available at https://authorea.com/users/890168/articles/1267414-a-high-frequency-ac-generator-with-high-gain-powered-by-3-7-v-battery-for-tumor-treating-fields

Fig. 5 (a) The maximum output voltage of the proposed resonant converter, at an input of 3.7 V. (f) Input voltage and current. (g) Output voltage and current. (h) Voltage amplitude before and after adjustment under different loads (i) The percentage of each harmonic of the output voltage. (j) The current decay curve as a function of battery runtime.

Fig. 5a shows the output waveform of the LCLLC resonant tank with an input voltage of 3.7 V. Using a 3.7 V DC battery and a transformer inductance of 10 μH, the output voltage reaches 66.0 V, meeting the requirements for tumor treatment. Generally, an output voltage of 50.0 V is sufficient for this purpose, so it was set to ˜50.0 V with a DC-DC converter for further analysis.

Figs. 5b and 5c show the DC input voltage and current, as well as the output voltage and current, respectively. The average input current reaches 1350 mA, with a total input power of 5.1 W, closely matching the simulation results. The output current can reach 960 mA, and the total average output power can reach 27.2 W, demonstrating that an input power of ˜5 W is sufficient for TTFields treatment.

In simulation analysis, the capacitive impedances of 60, 75, 90 Ω for TTFields treatment with 200 kHz. This study also chooses capacitor load impedance of 60, 75, 90 Ω, respectively. Fig. 5d shows the voltage outputs V_{out} with and without transformer adjustment. For LCLLC structure with capacitive impedances of 75 Ω, the output V_{out} is 51.3 V with the transformer inductance (8 μ H). The output V_{out} could reach to 50.0 V with the transformer inductance (5 μ H) for the capacitive impedances of 60 Ω.

Fig. 5e shows the comparison of harmonics (1st–11th) of the experimental waveform for proposed LCLLC resonant converter with impedance of 90 Ω. High harmonic distortion (THD) is only 1.4% of the output waveform, which is low enough for tumor treatment.

Fig. 5f shows the battery discharge current curve using four 18650 cells (3200 mAh) as the DC power supply. As mentioned in the Introduction, the output current of the clinical apparatus ranges from 400 mA to 1000

mA. This study uses 700 mA as the standard to test the effective output duration, ensuring that the output current does not fall below 630 mA (10%). Fig. 5f indicates that this design maintains a voltage of 50 V or more for 8.7 hours of continuous operation. For the Optune apparatus, patients require an additional battery or power supply if they plan to be away from home for more than one hour. The TTFields system requires a battery power of approximately 50.0 W. As shown in Fig. 5b, the average input power is only 5.1 W, which meets the requirements for both output voltage and current. Fig. 5f demonstrates that the LCLLC structure enables long-term outdoor TTFields treatment.

Materials & Methods on Cell Experiments

Cell culture

U251 glioma cells was purchased from Qingqi Biotechnology Development Co., Ltd. (Shanghai, China). U251 cells were cultured in RPMI-1640 complete medium (containing 100 U/mL penicillin and 100 U/mL streptomycin, 10% inactivated fetal bovine serum) at 37 under 5% CO_2 in the culture dish. The cell suspension was prepared with 2 mL of 0.25% trypsin-EDTA when 80% confluency was reached. After two minutes, 2 mL of 1640 medium was added to inactivate trypsin-EDTA and centrifuged at 800 rpm for 5 minutes at room temperature. Then, the supernatant was discarded, and the cell culture was re-suspended, configuring to a cell suspension with 1×10^5 cells/mL. The cell suspension was were seeded into each well of six-well plates with 1 mL. After twelve hours, the cells were treated by high frequency AC field.

Experimental setups

The insulated electrode sheet (Fig. 6a) was designed to deliver high frequency AC field. The insulated electrode consists of a PCB board, insulating ceramic sheet, and silica gel, where the PCB board was designed to provide support and connection between electrode and generator. The top pad of the PCB board connected to the power output, while the bottom pad was linked to the ceramic sheet via conductive silver paste, with silica gel filling the gap to prevent direct contact between the conductive parts and the cell culture medium. The PCB board measures 25.24 mm in length, 1.6 mm in width, and 19 mm in height. The distance between the two electrode sheets in the six-well cell culture plate is 20.18 mm. The dimensions of the ceramic sheet are 19.05 mm × 9.53 mm × 0.2 mm. A PCB holder was designed to secure six electrode plates in the six-well cell culture plate, allowing three sets of experiments to be conducted simultaneously. Thin wires connected the power supply to the PCB holder, ensuring the six-well cell plate remained sealed, thus providing an uncontaminated environment for the cells (Fig. 6b). The experimental setup is shown in Fig. 6c.

Hosted file

`image47.emf` available at https://authorea.com/users/890168/articles/1267414-a-high-frequency-ac-generator-with-high-gain-powered-by-3-7-v-battery-for-tumor-treating-fields

Fig. 6 (a) The insulating electrode sheet. (b) The electric field applied partial device. (c) High frequency electric field generator experimental setup.

Cell Viability

The high frequency AC field with 200 kHz was applied to U251 cells for 24 h, and 48 h respectively. An oscilloscope (Teledyne Lecroy, WS3034), a Teledyne LeCroy PP020 passive probe and a Pearson Current probe (Model 6600, Pearson Electronics, Inc., Palo Alto, CA, USA) were used to measure the voltage and current during the experiments. After the stimulation, 1 mL of 1640 medium was added to inactivate trypsin-EDTA and centrifuged at 800 rpm for 5 minutes. Then the supernatant was discarded, and 1mL new 1640 medium was added in the cell suspension. Subsequently, the cell suspension was transferred into 96-well

plates (100 μL/well). 20 μL of CCK-8 (Dojindo, Japan) was added to each well of the 96-well plate, and the incubation was continued for 1 hour at 37 . Finally, the absorbance of cells was analyzed by a microplate reader (H1-Synergy, USA). Cell viability was calculated from the absorbance of cells both in the treated and control groups. The experiments were performed three times at least.

Establishment and Feasibility Analysis of Finite Element Simulation

Before the cell experiment, a proportional simulation model was built using COMSOL Multiphysics to verify the feasibility of the experimental scheme. The relative dielectric constants and conductivity parameters used in the simulation model are shown in Table 3.

Table 3 Simulation Parameters of the Devices in the Cell Plate

Materials	Conductivity	Relative permittivity constanct
Cell plate	1×10^{-15}	3.7
Cell culture medium	1.5	80
Insulating ceramics	0	25000
PCB substrate	1×10^{-12}	4.5
Air	0	1
Pad	5.998×10^{7}	1

In the simulation, one well of the six-well cell culture plate was analyzed by applying a 200 kHz AC signal with a peak value of 5 V to the pad conductors on both sides of the well. Fig. 7a shows the model built in the software, and Fig. 7b presents a cross-sectional view of the field strength distribution in the cell culture medium when a peak 5 V AC signal is applied to the two electrode plates.

In general, the dielectric constant of ceramic section of electrode could significantly affect electric field distribution. Therefore, we firstly simulated the electric field distribution with different dielectric constant of ceramic section. Figs. 7c-7f show the electric field distribution when AC field with 200 kHz and 5 V is applied. The results showed that the electric field distribution increases with higher dielectric constant of ceramic section. The area where intensity of electric field is over 1.5 V/cm also increases with higher dielectric constant of ceramic section, which is shown in Fig. 7g. Therefore, this study uses ceramic with dielectric constant of 25000 (the highest dielectric constant ceramic we found) for cell experiment.

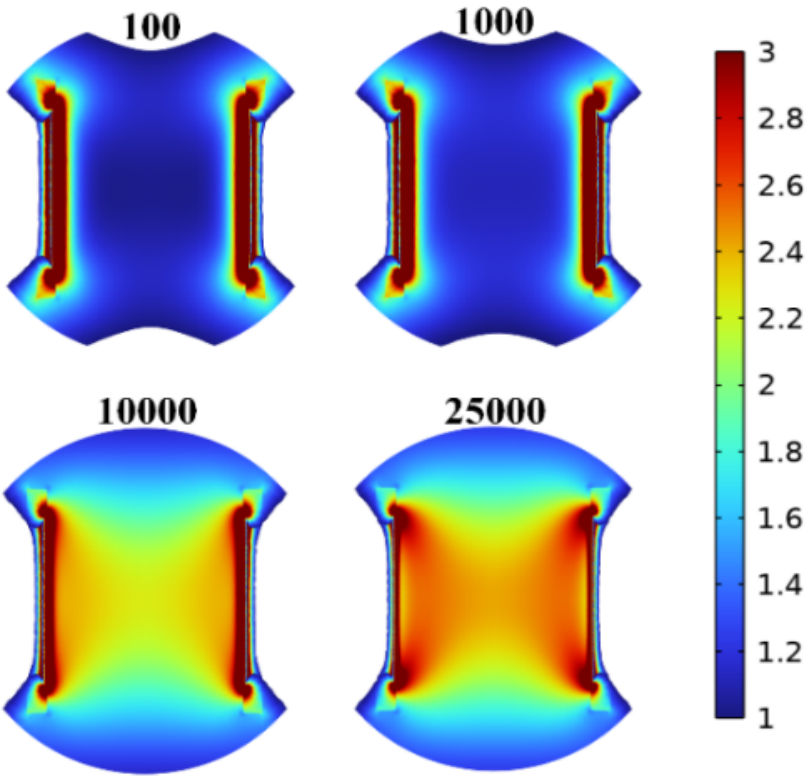

Fig. 7 (a) The constructed cellular experimental model. (b) The cross-sectional distribution of the electric field strength. (c)-(f) he electric field distribution by various dielectric constant of ceramic section (100, 1000, 10000, 25000) when AC field with 200 kHz and 5 V is applied. (g) The percentage of area where electric field distribution is above 1.5 V/cm by various dielectric constant of ceramic section (100, 1000, 10000, 25000).

Results on Cell Viability

In order to improve the calculation accuracy of electric field distribution, we measure the current waveforms during cell experiments (Fig. 8a) to match the simulation current. The voltage of AC field is 5 V, the experimental current peak could reach to 43 mA. The simulated current is 40 mA, which is similar with the experimental current. The simulation shows that the field strength distribution between the two electrode ranges from 2.0 V/cm to 3.0 V/cm (Fig. 7d). The average electric field strength is 2.38 V/cm.

Fig. 8b shows the representative U251 cell morphology of the control and experimental groups at 24 h, and 48 h, after treatment. For control group, U251 cells shows an elongated morphology at 24 h, which indicates that U251 cells grow well. For 48 h, U251 cells grow rapidly, compared with 24 h. For experimental groups, some cells show a round-like morphology (blue arrow), at 24 h after treatment. Moreover, the cell density is lower than control group. At 48 h after treatment, more round-like cells occur on the experimental groups. The cell density is significantly lower, compared with 48 h control group. Fig. 8c shows the cell viability at 24 h, and 48 h, after treatment. The cell viability of experimental group (85.1±5.8%) at 24 h is significantly lower than that by control group. At 48 h, the cell viability of experimental group (70.2±4.5%) is further lower that by control group. Figs 8a and 8b show that the designed high frequency AC generator could inhibit cell proliferation significantly

Hosted file

image55.emf available at https://authorea.com/users/890168/articles/1267414-a-high-frequency-ac-generator-with-high-gain-powered-by-3-7-v-battery-for-tumor-treating-fields

Fig. 8 (a) Voltage-current waveforms in cell experiments. (b) Cellular morphology of control and experimental groups at 24 h and 48 h after treatment. Blue arrow represents the round cell. (c) The cell viability at 24 h, and 48 h, after TTFs treatment.

Conclusion

This paper designed a high frequency AC generator (200 kHz) power by 3.7 V DC lithium battery for application of tumor treating field. The following conclusions can be derived: 1) The LCLC step-up resonant with 1:1 linear transformer (LCLLC) was proposed to boost the voltage. Based on the theoretical analysis, with proper selection of excitation inductances of linear transformer, the LCLLC step-up resonant could shift resonant gain frequency to the targeted frequency (200 kHz), then achieve a high voltage gain. With a large range of excitation inductances, the resonant frequency changes in a relatively narrow change, which indicates that it is a proper way to select adaptive excitation inductance of transformer for fine tuning of targeted frequency to resonant frequency. 2) A prototype powered by 3.7 V DC lithium battery is designed to output high frequency AC field (200 kHz). The designed generator could output 66 V AC field (200 kHz) with a voltage gain of 17.8 (3.7 V DC supply). For bio-load impedances of 60, 75, and 90 Ω, the excitation inductances of linear transformer were properly selected to achieve same output voltage (50 V). The prototype could sustainably run for about 8 hours when powered by four 3.7 V lithium batteries (5.1 W). 3) The finite element model was used to simulate electric field distribution with designed insulated electrodes. The results showed that high dielectric constant of ceramic section of electrode could contribute to deliver electric field to targeted region. The *in vitro* cell experimental indicates that the designed prototype could output proper AC field with 200 kHz by designed insulated electrodes to inhibit cell proliferation significantly.**Acknowledgements** This work was supported in part by the National Natural Science Foundation of China under Grant 52007172, in part by the China Postdoctoral Science Foundation under Grant 2020M672273, in part by Henan Province Scientific Research Joint Fund Industrial Category Major Program under Grant 245101610001, in part by Natural Science Foundation of Henan Province under Grant 222300420538.**Author Contributions Yanpeng Lv: Conceptualization, Investigation, Supervision, Methodology, Project administration. Shihan Lu Software, Writing-original draft. Yuqi Wang:** Analyzed data, Debugging prototype**Xuan Liu:** Design experiments. **Jianhua Zhang: Data curation, Visualization, Writing-review & editing.**

Declaration

Conflict of interests the authors declare that they have no known competing financial interests or personal.

Reference

1. Stupp, R., Wong, E. T., Kanner, A. A., Steinberg, D., Engelhdard, H., Kirson, E. D., et al. (2012). NovoTTF-100A versus physician's choice chemotherapy in recurrent glioblastoma: a randomised phase III trial of a novel treatment modality. Eur. J. Cancer. 48, 2192–2012. doi: 10.1016/j.ejca.2012.04.011.
2. Stupp, R. et al. Effect of tumor-treating fields plus maintenance temozolomide vs maintenance temozolomide alone on survival in patients with glioblastoma: a randomized clinical trial. JAMA 318, 2306–2316 (2017).
3. MUN E J, BABIKER H M, WEINBERG U, et al. Tumor-treating fields: a fourth modality in cancer treatment [J]. Clinical Cancer Research, 2018, 24(2): 266-275.

4. Kanner, A. A., Wong, E. T., Villano, J. L., and Ram, Z. (2014). Post hoc analyses of intention-to-treat population in phase III comparison of NovoTFF-100A system versus physician's choice chemotherapy. Semin. Oncol. 41, S25–S34. doi: 10.1053/j.seminoncol.2014.09.008.
5. Kirson, E. D., Dbalý, V., Tovarys, F., Vymazal, J., Soustiel, J. F., Itzhaki, A., et al. (2007). Alternating electric fields arrest cell proliferation in animal tumor models and human brain tumors. Proc. Nat. Acad. Sci. 104, 10152–10157. doi: 10.1073/pnas.0702916104.
6. Maintenance Therapy With Tumor-Treating Fields Plus Temozolomide vs Temozolomide Alone for Glioblastoma A Randomized Clinical Trial.
7. Miranda, P. C., Mekonnen, A., Salvador, R., and Basser, P. J. (2014). Predicting the electric field distribution in the brain for the treatment of glioblastoma. Phys. Med. Biol. 59, 4137–4147. doi: 10.1088/0031-9155/59/15/4137.
8. Killock, D. TTFields improve survival. Nat Rev Clin Oncol 15, 136 (2018). https://doi.org/10.1038/nrclinonc.2018.2.
9. Lok, E., Wong, E.T., Sajo, E. (2016). Computer Simulation of Tumor Treating Fields. In: Wong, E. (eds) Alternating Electric Fields Therapy in Oncology. Springer, Cham. https://doi.org/10.1007/978-3-319-30576-9_4.
10. Miranda, P. C., Mekonnen, A., Salvador, R., and Basser, P. J. (2014). Predicting the electric field distribution in the brain for the treatment of glioblastoma. Phys. Med. Biol. 59, 4137–4147. doi: 10.1088/0031-9155/59/15/4137.
11. Wenger, C., Salvador, R., Basser, P. J., and Miranda, P. C. (2015). The electric field distribution in the brain during TTFields therapy and its dependence on tissue dielectric properties and anatomy: a computational study. Phys. Med. Biol. 60, 7339–7357. doi: 10.1088/0031-9155/60/18/7339.
12. Gentilal, Nichal et al. "Temperature and Impedance Variations During Tumor Treating Fields (TTFields) Treatment." *Frontiers in human neuroscience* 16 (2022): 931818. Print.
13. L. Grajales and F. C. Lee, "Control system design and small-signal analysis of a phase-shift-controlled series-resonant inverter for induction heating," Proceedings of PESC '95 - Power Electronics Specialist Conference, Atlanta, GA, USA, 1995, pp. 450-456 vol.1, doi: 10.1109/PESC.1995.474849.
14. W. Reeve, "DC power system design for telecommunications," in IEEE Telecommunications Handbook Series. Hoboken, NJ, USA: Wiley, 2006.
15. H. Radwan, M. A. Sayed, T. Takeshita, A. A. Elbaset and G. Shabib, "A Novel Single- Stage High-Frequency Boost Inverter Cascaded by Rectifier-Inverter System for PV Grid-Tie Applications," 2018 International Power Electronics Conference (IPEC-Niigata 2018 -ECCE Asia), Niigata, Japan, 2018, pp. 3945-3951, doi: 10.23919/IPEC.2018.8507412.
16. M. A. Sayed, K. Suzuki, T. Takeshita and W. Kitagawa, "Soft-Switching PWM Technique for Grid-Tie Isolated Bidirectional DC–AC Converter With SiC Device," in IEEE Transactions on Industry Applications, vol. 53, no. 6, pp. 5602-5614, Nov.-Dec. 2017, doi: 10.1109/TIA.2017.2731738.
17. X. Hu, Y. Zhang, X. Liu, Z. Yu, T. He and L. Mao, "A Non-Isolated Step-up DC-AC Converter With Reduced Leakage Current for Grid-Connected Photovoltaic Systems," in IEEE Access, vol. 8, pp. 71907-71916, 2020, doi: 10.1109/ACCESS.2020.2986605.
18. B. Zhang, P. Yang, Q. Ge, X. Wang and Y. Li, "A New High Output Frequency Multilevel Inverter Topology of Traction Converter for Superspeed Maglev Train," 2021 13th International Symposium on Linear Drives for Industry Applications (LDIA), Wuhan, China, 2021, pp. 1-5, doi: 10.1109/LDIA49489.2021.9505946.
19. W. Song, S. Jiao, Y. W. Li, J. Wang and J. Huang, "High-Frequency Harmonic Resonance Suppression in High-Speed Railway Through Single-Phase Traction Converter With LCL Filter," in IEEE Transactions on Transportation Electrification, vol. 2, no. 3, pp. 347-356, Sept. 2016, doi: 10.1109/TTE.2016.2584921.
20. E. Rasool and M. Darwish, "High frequency inverter circuit for UPS systems," 2012 47th International Universities Power Engineering Conference (UPEC), Uxbridge, UK, 2012, pp. 1-4, doi: 10.1109/UPEC.2012.6398602.
21. A. T. L. Lee, W. Jin, S. -C. Tan and S. Y. Hui, "Buck-Boost Single-Inductor Multiple-Output High-

Frequency Inverters for Medium-Power Wireless Power Transfer," in IEEE Transactions on Power Electronics, vol. 34, no. 4, pp. 3457-3473, April 2019, doi: 10.1109/TPEL.2018.2855678.
22. F. M. Ibanez, "Bidirectional Series Resonant DC/AC Converter for Energy Storage Systems," in IEEE Transactions on Power Electronics, vol. 34, no. 4, pp. 3429-3444, April 2019, doi: 10.1109/TPEL.2018.2854924.
23. K. Kanathipan and J. Lam, "An Electrolytic Capacitor-Less PV Micro-Inverter Based on CLL Resonant Conversion With a Power Control Scheme Using Resonant Circuit Voltage Control Loops," in CPSS Transactions on Power Electronics and Applications, vol. 7, no. 2, pp. 139-149, June 2022, doi: 10.24295/CPSSTPEA.2022.00013.
24. A. Ray and K. Rajashekara, "Design and Evaluation of a High Current Gain Resonant Inverter for Subsea Electrical Heating," in IEEE Transactions on Industry Applications, vol. 58, no. 4, pp. 5093-5103, July-Aug. 2022, doi: 10.1109/TIA.2022.3172392.
25. Chien-Ming Wang and Guan-Chyun Hsieh, "A series-resonant DC/AC inverter for impedance-load drives," in IEEE Transactions on Power Electronics, vol. 16, no. 3, pp. 325-335, May 2001, doi: 10.1109/63.923764.
26. X. Li and A. K. S. Bhat, "A Utility-Interfaced Phase-Modulated High-Frequency Isolated Dual LCL DC/AC Converter," in IEEE Transactions on Industrial Electronics, vol. 59, no. 2, pp. 1008-1019, Feb. 2012, doi: 10.1109/TIE.2011.2158044.
27. A. Blinov et al., "High Gain DC–AC High-Frequency Link Inverter With Improved Quasi-Resonant Modulation," in IEEE Transactions on Industrial Electronics, vol. 69, no. 2, pp. 1465-1476, Feb. 2022, doi: 10.1109/TIE.2021.3060657.
28. N. Kummari and S. Chattopadhyay, "Three-Legged High-Gain Phase-Modulated DC–AC Converter for Mitigation of Device Capacitance Induced Ringing Voltage," in IEEE Transactions on Power Electronics, vol. 35, no. 2, pp. 1306-1321, Feb. 2020, doi: 10.1109/TPEL.2019.2918737.
29. N. Kummari, S. Chakraborty, and S. Chattopadhyay, "An isolated highfrequency link microinverter operated with secondary-side modulation for efficiency improvement," IEEE Trans. Power Electron., vol. 33, no. 3, pp. 2187–2200, Mar. 2018.
30. H. Wu, Y. Jia, F. Yang, L. Zhu, and Y. Xing, "Two-Stage isolated bidirectional DC–AC converters with three-port converters and two DC buses," IEEE J. Emerg. Sel. Top. Power Electron., vol. 8, no. 4, pp. 4428–4439, Dec. 2020.
31. Instructions for Use for Unresectable MalignantPleural Mesothelioma. https://www.optunelua.com/pdfs/Optune-Lua-MPM-IFU.pdf
32. Murphy, Janlyn, Mary Ellen Bowers, and Loretta Barron. "Optune(r): Practical Nursing Applications." *Clinical journal of oncology nursing* 20.5 (2016): 14–19. Print.
33. Lang ST, Gan LS, McLennan C, Monchi O, Kelly JJP. Impact of Peritumoral Edema During Tumor Treatment Field Therapy: A Computational Modelling Study. IEEE Trans Biomed Eng. 2020 Dec;67(12):3327-3338. doi: 10.1109/TBME.2020.2983653. Epub 2020 Nov 19. PMID: 32286953.
34. Stupp, Roger et al. "NovoTTF-100A versus physician's choice chemotherapy in recurrent glioblastoma: a randomised phase III trial of a novel treatment modality." European journal of cancer (Oxford, England : 1990) vol. 48,14 (2012): 2192-202. doi:10.1016/j.ejca.2012.04.011.
35. H. Y. Lu, J. G. Zhu, and S. Y. R. Hui, "Experimental determination of stray capacitances in high frequency transformers," IEEE Trans. Power Electron., vol. 18, no. 5, pp. 1105–1112, Sep. 2003.
36. C. W. T. McLyman, Transformer and Inductor Design Handbook, Fourth Edition. CRC Press, 2016.
37. Yin,Shan,et al."A 1-MHz GaN-Based LCLC Resonant Step-Up Converter With Air-Core Transformer for Satellite Electric Propulsion Application".IEEE Transactions on Industrial Electronics,vol.69,2022,pp.11035-11045,https://doi.org/10.1109/TIE.2021.3121711.